Article

DEVELOPMENT OF A DRUG DELIVERY SYSTEM BASED ON CHITOSAN NANOPARTICLES FOR ORAL ADMINISTRATION OF INTERFERON-ALPHA.

Camila Cánepa, Julieta Celeste Imperiale, Carolina A. Berini, Marianela Lewicki, Alejandro Sosnik, and Mirna M. Biglione

Biomacromolecules, **Just Accepted Manuscript** • DOI: 10.1021/acs.biomac.7b00959 • Publication Date (Web): 24 Aug 2017

Development of a drug delivery system based on chitosan nanoparticles for oral administration of interferon-alpha

Camila Cánepa[1], Julieta C. Imperiale[2], Carolina A. Berini[1], Marianela Lewicki[3], Alejandro Sosnik[4]‡ & Mirna M. Biglione[1]‡.*

[1] CONICET - Universidad de Buenos Aires. Instituto de Investigaciones Biomédicas en Retrovirus y Sida (INBIRS). Buenos Aires, Argentina.

[2] CONICET - Universidad de Buenos Aires. Instituto de Investigaciones Farmacológicas (ININFA). Buenos Aires, Argentina.

[3] CONICET - Universidad de Buenos Aires. Instituto de Investigaciones en Microbiología y Parasitología Médica (IMPAM).

[4] Laboratory of Pharmaceutical Nanomaterials Science, Department of Materials Science and Engineering, Technion-Israel Institute of Technology, Technion City, Haifa, Israel.

ABSTRACT. Despite the good clinical efficacy of interferon alpha (IFNα) to treat some types of cancer and viral infections, this biological drug is underused given its severe adverse effects and high dosing parenteral regimens. Aiming to achieve a breakthrough in the therapy with IFNα, this work reports for the first time on the design and full characterization of a novel nanomedicine of IFNα-2b-loaded chitosan nanoparticles (IFN-CT NPs) for oral delivery. IFN-CT NPs produced by ionotropic gelation encapsulated approximately 100% of the drug, showed a size of 36 ± 8 nm, a zeta-potential of +30 mV (dynamic light scattering) and a spherical morphology (transmission electron microscopy). The antiviral activity of IFN-CT NPs *in vitro* was comparable to the commercial IFNα. Remarkably, both treatments stimulated the expression of IFN genes to a similar extent in both non-infected and infected cells with the Human Lymphotropic-T Virus type 1 (HLTV-1). Finally, oral administration of IFN-CT NPs (0.3MIU) to CF1 mice showed detectable levels of IFNα in plasma after 1 h, while no IFNα was detected with a commercial formulation. These results are encouraging and open a new avenue for the administration of this biological drug in a minimally-invasive, safer and more patient-compliant way.

KEYWORDS. Interferon alpha; nanomedicine; chitosan nanoparticles; oral delivery.

INTRODUCTION

Protein- and peptide-based biological drugs are increasingly positioned in the pharmaceutical market. However, these therapeutics usually have high molecular weight, low lipophilicity and the presence of charged groups constrain their absorption by non-parenteral routes. In addition, luminal, brush border and cytosolic metabolism, as well as hepatic clearance result in poor bioavailability for oral delivery. Hence, protein-based drugs are usually administered by injection[1]. Notwithstanding, the oral route is the most preferred because it enables self-administration, it is more patient-compliant and it reduces costs associated with sophisticated sterile manufacturing facilities and processes[2]. Currently, there are several strategies aimed to increase the oral bioavailability of biological drugs including structural modifications, enzyme inhibitors, and absorption enhancers.

Nanotechnology has emerged as a promising tool to deliver proteins and peptides by the oral route[3-5]. Nonetheless, there are still many challenges to translate this vision into the clinical practice[4,6]. In this scenario, most of the investigative efforts have been devoted to insulin[7-9], and with less emphasis to calcitonin, human granulocyte colony stimulating factor[10], cyclosporine[11] and vasopressin[12]. The appropriate approach should not only protect the protein/peptide from chemical and/or enzymatic degradation in the gastrointestinal tract but also aid in enhancing its absorption across the intestinal epithelium, without jeopardizing its biological activity[13].

Interferon alpha (IFNα, INTRON® A, Merck & Co., Inc.) is a protein used to treat different types of cancer (e.g., hairy cell leukemia, malignant melanoma, AIDS-related Kaposi's sarcoma, follicular non-Hodgkin's lymphoma and condyloma acuminata) and viral

infections, as it regulates the expression of many genes involved in the suppression of cell proliferation *via* Janus kinase/Signal Transducer and Activator of Transcription signaling pathway and the inhibition of viral replication[14]. Given its short half-life and narrow therapeutic index, IFNα is injected in high dose and frequent regimens[15]. This is associated with pain and allergic reactions which have a strong impact on patient compliance. Moreover, it causes severe dose-dependent adverse effects that limit its use. Aiming to overcome these drawbacks, a pegylated form of IFNα (PEG-IFNα) that prolongs its half-life and enables a once-a-week injection was developed. However, adverse effects persist and the modified drug demonstrated a dramatic decrease of up to 2000-fold in the biological activity *in vitro* when compared to the unmodified counterpart[16]. Nonetheless, PEG-IFNα is still considered the gold-standard along with zidovudine to treat acute and favorable chronic Adult T Cell Leukemia (ATL), a pathology caused by the retrovirus Human Lymphotropic T Virus Type 1 (HTLV-1) because response rates and survival are higher than with standard chemotherapy[17].

A number of advanced nano-drug delivery systems have been recently described for IFNα, ranging from polymeric and gold nanoparticles to silicon channels[18,19]. However, these investigations did not contribute to change the administration strategy that represents a major concern in IFN therapy. To the best of our knowledge, the only work in this direction reported on the encapsulation of IFNα within microparticles of trimethyl-chitosan, poly(ethylene glycol) dimethacrylate and methacrylic acid. Nevertheless, a relatively low loading efficiency (53.25%) was achieved, precluding the bench-to-bedside translation[20].

Aiming to make a significant contribution to the therapy with IFNα, in this work we describe the design and full characterization of a novel nanomedicine of IFNα-2b-loaded chitosan nanoparticles (IFN-CT NPs) with an encapsulation efficiency of approximately 100% for oral administration. After demonstrating the antiviral activity of nano-encapsulated IFNα *in vitro*, we administered one single dose of IFN-CT NPs (0.3MIU) to CF1 mice and showed detectable levels in plasma after 1 h, as opposed to the free drug that was undetectable. To our knowledge, no similar results in animal models have been reported before. This may represent a step forward in the administration of this biological drug in a minimally-invasive, safer and more patient-compliant way.

EXPERIMENTAL SECTION

Materials

Low molecular weight 82.6% deacetylated chitosan (CT) and sodium tripolyphosphate pentabasic (TPP) were supplied by Sigma-Aldrich (USA). Acetic acid was purchased from Merck (Germany) and IFNα-2b (BIOFERON®, lyophilized powder) from BioSidus (Argentina).

Preparation of IFNα-loaded chitosan nanoparticles (IFN-CT NPs)

IFN-CT NPs were prepared by the ionotropic gelation method between the polycationic CT and TPP anions. For this, CT was dissolved in acetic aqueous solution (3.5 mg/mL) under magnetic stirring (2 h), alkalinized to pH 5.5, and filtered (0.45 μm nitrocellulose membrane, Osmonics Inc., USA).

IFN-CT NPs were spontaneously formed by the dropwise addition of TPP (1.8 mL, 1 mg/mL in water) to a CT solution (4.5 mL, 2 mg/mL) containing IFNα (24 μg, equivalent to 5 MIU/batch) using a 21G1 1/2 needle (internal diameter = 0.80 mm, length = 38 mm) and an infusion pump (flow of 15 mL/h, PC11U, APEMA S.R.L., Argentina) under magnetic stirring, at room temperature. The nanosuspension was magnetically stirred (15 min) at room temperature to consolidate the crosslinking. For the preparation of IFN-free CT NPs (control), a similar procedure was used, though without the addition of the drug. Unreacted CT was quantified by a colorimetric method described elsewhere, with a slight modification[21]. For this, a calibration curve was built by mixing CT aliquots (2 mg/mL, pH 5.5) of 15, 30, 45, 60, 80, 100, 150, 200 and 250 μL with the corresponding volume of phosphate buffer (pH 5.5), to complete a final volume of 300 μL. An alizarinsulfonic acid dye solution (3 mL, 0.5 mg/mL, pH 5.5) was added to each one. The absorbance was measured by UV-Visible spectrophotometry at λ = 551 nm. Then, to quantify the amount of free CT in the batch of NPs, a sample (300 μL) was extracted and subjected to the same procedure.

Characterization of the NPs

Particle size, size distribution and zeta-potential. The particle size (hydrodynamic diameter, D_h) and size distribution (polydispersity index, PDI) of the unloaded and IFNα-loaded NPs was measured by dynamic light scattering (DLS, Zetasizer Nano-ZS, Malvern Instruments, UK), provided with a He–Ne (633 nm) laser and a digital correlator ZEN3600 using an angle of θ = 173° to the incident beam, at 25°C. Results are expressed as number-based distribution of three samples prepared under identical conditions and each one of

them is the result of at least four runs. The zeta-potential of the different NPs was measured using the same equipment in fresh samples (pH 5.5, conductivity 2.2 μmcm/Vs).

Morphology. The morphology of the NPs was visualized by transmission electron microscopy (TEM, Zeiss EM109T, Germany). Samples were casted on copper grids, dried at room temperature and examined without previous staining. Additionally, for NP size confirmation, TEM images of three independent batches were analyzed by ImageJ Software v1.49 (National Institutes of Health, USA).

Infrared spectroscopy. CT, TPP and CT NPs were characterized by attenuated total reflectance Fourier transform infrared spectroscopy (ATR/FTIR, Nicolet 380 ATR/FTIR spectrometer, Avatar Combination Kit, Thermo Scientific, USA) by using Smart Multi-Bounce HATR with reflection ATR ZnSe crystal and an angle of 45° and recorded in a scanning range of 500–4000 cm^{-1}, with resolution of 4 cm^{-1} and 32 scans. For this, a CT solution in acetic acid as well as the nanosupension were freeze-dried prior to characterization. Spectra were obtained using the OMNIC 8.3 spectrum software (Thermo Scientific).

Encapsulation efficiency of IFNα. The encapsulation efficiency (*%EE*) of IFNα was indirectly determined by quantifying free IFNα in the supernatant of three independent batches of NPs produced under identical conditions by a commercial enzyme-linked immunosorbent assay kit (ELISA, Affimetrix, EBiosciences, USA). The *%EE* was calculated according to Equation 1

$$\%EE = [(D_o - D_f) / D_o] \times 100 \qquad (1)$$

Where D_o is the total amount of IFNα used in the preparation of the NPs and D_f is the amount of free IFNα measured in the supernatant after the encapsulation stage.

Mucoadhesion *in vitro*

The mucoadhesion of CT NPs *in vitro* was estimated by the mucin solution method that is based on changes of D_h and zeta-potential due to the agglomeration of NPs with mucin[22]. For this, mucin (Sigma-Aldrich) was dissolved in an HCl solution (pH 5.5) with 140 mM NaCl (Anedra, Argentina) and 5 mM KCl (Anedra). Then, equal volumes of mucin (1 mg/mL) and CT NPs (0.25 mg/mL) were mixed, vortexed for 30 s and incubated in a thermostated bath (Vicking Masson, Argentina), at 37 °C (2 h). Then, the D_h, PDI and zeta-potential of nanoparticles immersed in the mucin solution were followed up by DLS using the same method described to characterize fresh NPs (see above) and compared to the original CT NPs. Assays were conducted in triplicate and results are expressed as the mean ± S.E.M. Data for each single sample were the result of at least five runs. Statistical analysis was conducted by paired t-test, using GraphPad Prism 6.01v (GraphPad Software, Inc., USA).

***In vitro* release of IFNα**

In vitro release studies were conducted in 1N HCl solution and in phosphate buffer pH 6.8 containing 0.2% w/v Tween® 20 in order to simulate gastric and intestinal medium, respectively. The surfactant was added to prevent adsorption of IFNα to the surface of the container[23]. Briefly, a complete IFN-CT NP batch (6.8 mL) was poured directly into the release media. At predetermined time points, aliquots (1 mL each) were withdrawn and

replaced by the same volume of fresh pre-heated medium. The amount of IFNα was measured by ELISA (see above). Assays were carried out in triplicate and the results are expressed as mean ± S.E.M.

Biological activity *in vitro*

Cells lines. A bovine kidney cell line, MDBK (ATCC, USA), was maintained in DMEM medium (Life Technologies, Inc., USA) containing 10% fetal calf serum (FCS, Sigma-Aldrich) and antibiotic-antimycotic solution (AAS, Sigma-Aldrich).

Patient cells. Peripheral blood of healthy volunteers and HTLV-1 infected patients were obtained under written informed consent, and immediately used for the experiments. A brief description of each patient clinical status is shown in **Table S1**. Peripheral blood mononuclear cells (PBMCs) were isolated by Ficoll-Hypaque technique (GE Healthcare Life Sciences, USA). Cells were maintained in RPMI 1640 medium (Life Technologies) containing 10% FCS, AAS, 30–100 IU/mL of recombinant human IL-2 (Shionogi, Japan) and when required, stimulated with 10 ng/mL of phorbol 12-myristate 13-acetate (PMA, Sigma-Aldrich) before IFNα treatment.

Antiviral activity against Vesicular Stomatitis Virus (VSV). The antiviral activity of IFN-CT NPs against VSV was determined by measuring the inhibition of the cytopathic effect on MDBK cells. This technique is codified in the European Pharmacopeia and it is a market requirement for commercial IFNα[24]. Cells were treated with commercial reconstituted BIOFERON® (250 UI/mL IFNα), IFN-CT NPs (250 UI/mL IFNα, 60 μg/mL CT) or CT NPs (60 μg/mL CT). After incubation with the corresponding treatment and further

infection (multiplicity of infection was 0.1), cells were fixed and stained with crystal violet. Absorbance was measured at 590 nm and that of control cells was considered 100% viability. In a similar study, viable cells were quantified by CellTiter 96® AQueous Non-Radioactive Cell Proliferation Assay (MTS, Promega, USA). ANOVA test was used for data analysis; $p < 0.05$ was considered as statistically significant (GraphPad Prism 6.01v).

Antiviral activity against HLTV-1. Fresh PBMCs were cultured in 6-well plates (5 x 10^5/mL), PMA-stimulated, and treated with IFNα (100, 1000 or 10,000 UI/mL) for 24 h. Cells were centrifuged and pellets and supernatants used for the quantification of HTLV-1 Tax viral protein and p19 by flow cytometry and ELISA, respectively. For intracellular staining of Tax, cells were fixed with 4% paraformaldehyde (10 min) and permeabilized with a BD Perm/Wash™ Buffer Kit (BD Pharmingen, USA). Alexa Fluor 488-conjugated Lt-4, a mouse monoclonal antibody (mAb) against Tax (gently provided by Dr. Y. Tanaka, Department of Immunology, School of Medicine, University of the Ryukyus, Japan), was used for its detection. Statistical analysis was performed in Graph Pad Prism 6.01v (ANOVA test, $p < 0.05$). The concentration of HTLV-1 p19 in the supernatants from PMA-stimulated cultures was measured using a RETRO-tek HTLV-1/II p19 antigen ELISA, according to the instructions of manufacturer (ZeptoMetrix Corp., USA).

Activation of IFNα signaling pathway. Total RNA was extracted by the phenol technique (Trizol reagent, Thermo Fisher Scientific) from PMA-stimulated PBMCs exposed to IFNα treatment (1000 UI/mL) for 4 h. Aliquots (2 μg) of RNA were subjected to reverse transcription (RT) with random primers followed by PCR using Power SYBR qPCR Mix (Thermo Fisher Scientific). The relative ratio of the mRNA of two IFNα response genes,

namely 2'-5'-oligoadenylate synthetase 1 (OAS1) and radical S-adenosyl methionine domain containing 2 (RSAD2), was quantified. Primer sets were the following: OAS1f TGCGCTCAGCTTCGTACTGA, OAS1r GGTGGAGAACTCGCCCTCTT, RSAD2f GTGGTTCCAGAATTATGGTGAGTATTT, RSAD2r CCACGGCCAATAAGGACATT. The thermal cycling program involved an initial denaturation at 95°C for 20 s, then 40 cycles of denaturation at 95°C for 1 s, annealing and extension at 60°C for 20 s, and a final melt curve stage. The run was performed in a StepOnePlus™ System (Thermo Fisher Scientific). Products were quantified and normalized to the expression level of untreated cells and standardized against GAPDH (OAS1) and 18s (RSAD2) RNA copy numbers. Statistical analysis was performed in Graph Pad Prism 6.01v (Dunnett's ANOVA test, $p<0.05$).

Preliminary *in vivo* assays

To preliminary assess the capacity of the NPs to ensure the oral delivery of the cargo, we conducted a one-time point assay. Seven-week old CF-1 female mice (Animal Facility of the Department of Microbiology, Parasitology and Immunology, Faculty of Medicine, University of Buenos Aires, Argentina) were orally administered with 400 μL (0.3 MIU) of either free (n = 5) or nanoencapsulated IFNα (n = 5), with a straight probe coupled to a tuberculin needle. Furthermore, three mice were used as negative control and thus, received an equal volume of phosphate buffer saline. One hour later, blood samples were taken by cardiac puncture, previous intraperitoneal administration of anesthesia: 150 mg/kg ketamine (Sigma-Aldrich) and 10 mg/kg xylazine (Sigma-Aldrich). Then, blood samples were centrifuged to isolate plasma, which was stored at -80°C until analysis. IFNα levels

were quantified by ELISA, according to the instructions of manufacturer (Affimetrix, EBiosciences). The methodology described here was conducted following international ethics standards for preclinical trials and the protocol was approved by the Institutional Committee for Care and Use of Experimental Animals (CICUAL) of the Faculty of Medicine of the University of Buenos Aires (Resolution #2609/2016).

RESULTS AND DISCUSSION

Given the fact that IFNα has a very short half-life *in vivo* (2-3 h IM/SC; 2 h IV) and a narrow therapeutic index, a pegylated form was developed, thus prolonging its half-life and enabling a once-a-week injectable administration. However, PEG-IFNα injections cause pain, allergic reactions and poor patient compliance. In this context, a change in the administration strategy would represent a breakthrough in the pharmacotherapy. We hypothesized that the encapsulation of IFNα within CT nanoparticles, a mucoadhesive polymer that displays high biocompatibility and biodegradability, would protect the drug from gastric degradation and improve its oral bioavalability with respect to the free counterpart. An additional advantageous feature of CT stems from its capacity to increase the uptake of macromolecules through the opening of the tight junctions in the intestinal epithelium[6].

Preparation and characterization of IFN-CT NPs

Considering that IFNα is a protein and that organic solvents might result in its denaturation, we used the ionotropic gelation method for the production of the nano-drug delivery system that is water-based, simple, reproducible, cost-viable and eventually scalable under an

industrial setting[25,26]. In addition, IFNα presents a pI value of approximately 5.9 that would favor its electrostatic interaction with positively-charged CT, ensuring maximum *%EE* (see below). Although there are not nano-drug delivery systems of IFN on the market yet with the exception of its pegylated forms, other types of drugs are approved and commercialized as nanopharmaceuticals[27]. To increase the chances of bench-to-bedside translation, we not only used a method for the production of the NPs that could be scaled up using semi-continuous or continuous technologies but also chose CT as the polymeric matrix because it is approved by the US-Food and Drug Administration as a natural food additive and classified as "Generally Regarded as Safe" (GRAS).

ATR/FTIR analysis of CT NPs showed the shifting of the band corresponding to N-H bending from 1556 to 1548 cm^{-1} with respect to pristine CT that could be attributed to the interaction between the amine group of CT and the phosphate anion of TPP (**Table 1**). In addition, bands at 1139 and 893 cm^{-1} that belong to P-O bending of TPP were also observed. Conversely, the weak band of P=O stretching of TPP at 1208 cm^{-1} was absent due to the low relative concentration of TPP.

Table 1. ATR/FTIR analysis of CT, TPP and unloaded CT NPs.

Band (cm^{-1})			**Assignment**
CT	**TPP**	**CT NPs**	
3410		3297	Overlapping of O−H and N−H stretching
1637		1637	C-O stretching of amide
1556		1548	N-H bending of amine
1406		1404	C-O stretching and O-H bending of alcohol
1338, 1152		1344, 1147	C-N stretching of amine
1021		1019	C-O stretching of ether
	1208		P=O stretching

1139, 893	1139, 893	P-O bending

DLS analysis demonstrated the very small size of the NPs: D_h of blank NPs was 47 ± 7 nm (PDI of 0.47, **Figure 1A**), while the size of IFN-CT NPs decreased to 36 ± 8 nm (PDI of 0.41, **Figure 1E**). In addition, the zeta-potential, an indicator of the surface charge, was approximately +30 mV for both unloaded and loaded nanoparticles (**Figure 1B** and **1F**, respectively), ensuring optimal physical stability of the colloidal system. Additionally, TEM images showed that both types of NPs are spherical, sizes being in very good agreement with those measured by DLS (**Figure 1C, 1G**). The slight decrease in size shown by IFN-CT NPs with respect to the unloaded counterparts most probably relied on the consolidation of a highly crosslinked polyelectrolyte network due to the interaction of the protein with the positively-charged CT matrix. Overall, these properties of size and surface charge would favor the retention of NPs in the intestine due to physical entrapment by the porous mucus layer and electrostatic mucoadhesion[28, 29].

The intrinsic mucoadhesive properties of CT have been extensively reported[11]. At pH values lower than the pK_a of CT, sialic acid residues in mucin – the main component of the mucus – interact with positively-charged amine groups through electrostatic interactions. While at greater pH values, the polymer interacts with mucin by hydrogen bonds. Thus, the adsorption of mucin molecules to the surface of the NPs would lead to an apparent increase in size as well as a masking of its surface charge and a consequent decrease of the zeta-potential. As expected, both blank and IFNα-loaded nanoparticles showed a significant increase in size after incubation in mucin solution reaching values of 273 ± 74 nm (**Figure 1D**) and 351 ± 12 nm (**Figure 1H**), respectively. Meanwhile, the surface charge decreased

to almost neutrality for both blank and IFNα- loaded nanoparticles (+2.1 ± 1.8 and -0.52 ± 1.3 mV, respectively). Zeta-potential values near to 0 mV increase the aggregation tendency of colloidal systems due to attractive inter-particle Van der Waals forces that contribute to increase the size of the NPs. These findings confirmed the mucoadhesiveness of CT NPs.

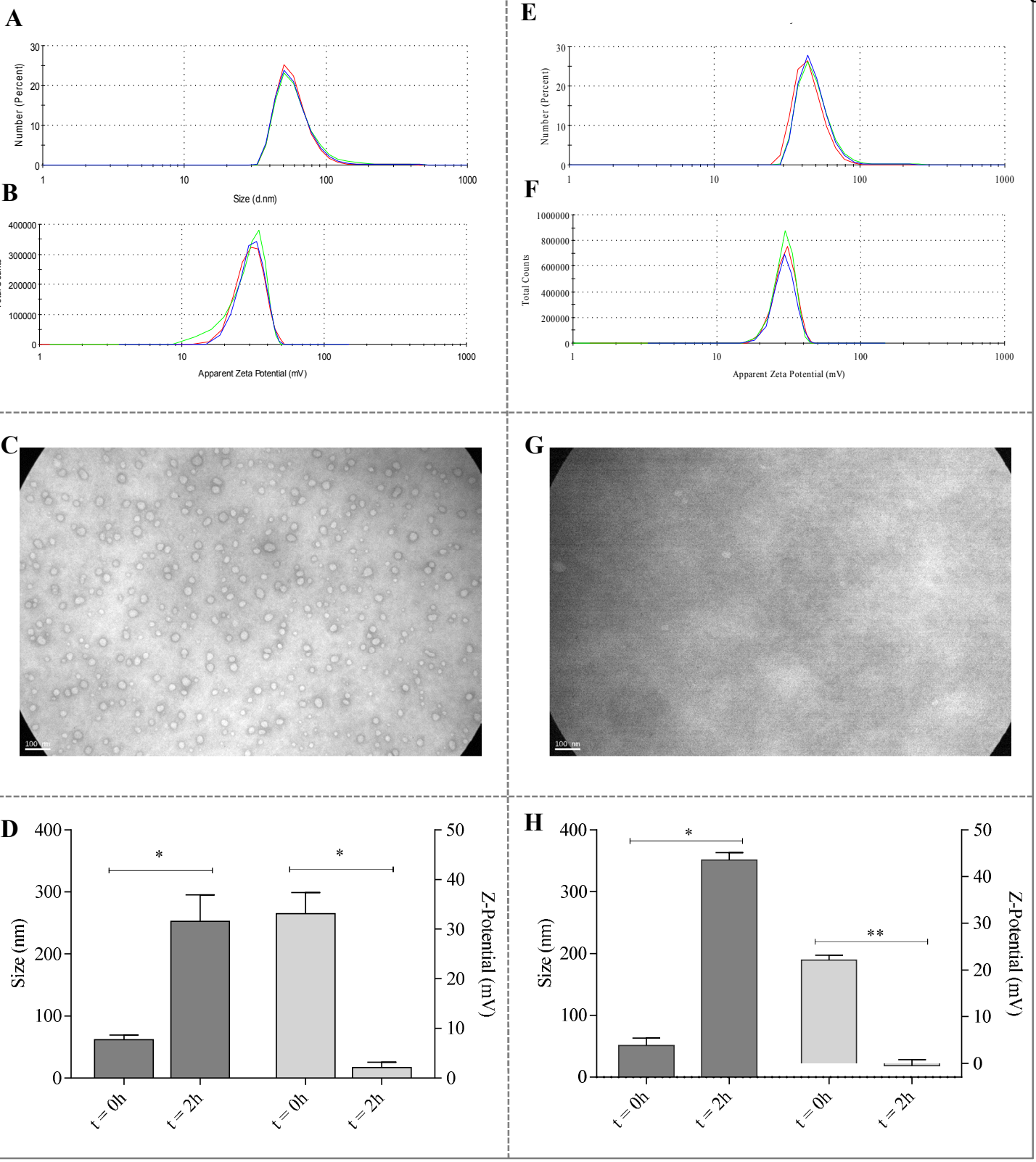

Figure 1. Characterization of the nanoparticles. (A,E) Size distribution, (B,F) zeta-potential distribution, (C,G) TEM micrographs and (D,H) mucoadhesive profile of blank

and IFNα-loaded nanoparticles. Results are expressed as mean ± S.E.M. Statistical significance is indicated as: *p <0.05 and **p <0.01.

The quantification of free CT and IFNα in the supernatant indicated that 95.5% of the total CT formed NPs and that 99.9% of the active molecule was encapsulated, resulting in a simple, reproducible and high-yield production process that could be eventually scaled up under an industrial setting.

In vitro release and stability of IFNα

Since the IFN-CT NPs developed in this work are conceived for oral administration, the release of IFNα under gastric- and intestine-like conditions was assessed. Results showed that 20.5 ± 0.6 % of drug was released after 30 min of contact in simulated gastric pH medium while, 89.6 ± 0.5 % of remaining drug was released within 30 min under simulated intestinal pH conditions (**Figure S1**). Considering that CT opens tight junctions and that probably some of the released drug could be interacting with the mucoadhesive polymer that is retained in the intestinal mucosa, the absorption could be facilitated.

Biological activity *in vitro*

After completing a thorough characterization of the NPs, we assessed the antiviral activity of the encapsulated protein and compared it with the free counterpart. It has been reported that after pegylation of IFNα-2a and IFNα-2b, only 7% and 28% of their antiviral activity *in vitro* is respectively conserved. As a direct consequence, IFNα doses must be increased with respect to the unmodified drug to achieve a similar therapeutic outcome. Considering

that adverse effects are dose-dependent, this might be one of the causes triggering them[30]. Moreover, the use of larger quantities of drug increases unit costs and makes the treatment unaffordable for patients in developing countries. Besides, it should be considered that the conjugation of PEG moieties is not a synthetic process deprived of technical hurdles, that demands substantial investment in manufacturing technology, resulting in a substantial increase of the production costs that translates into higher prices, especially for the production of sterile formulations[31].

Antiviral activity against VSV. The antiviral activity of IFN-CT NPs determined in VSV-infected cells was comparable to commercial IFNα (106.1 ± 4.3 and 104.7 ± 3.3%, respectively, $p > 0.9999$), while no activity was observed neither for the unloaded NPs nor for the CT solution (**Figure 2**). However, as some antiviral activity has been reported for CT[32], the experiment was repeated with a different read out method to confirm our results. In this case, different concentrations of a CT solution were also tested. No antiviral activity was detected for CT as solution or CT NPs (data not shown).

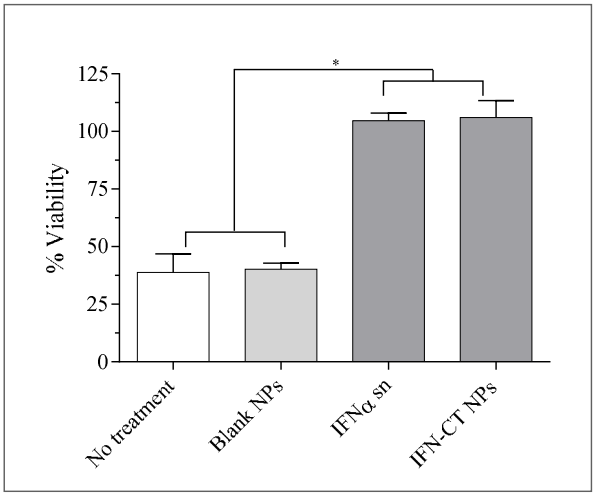

Figure 2. *In vitro* antiviral activity against VSV. Inhibition of cytopathic effect on MDBK cells was determined; absorbance of non-infected cells was set as 100% viability. Cells were treated with blank NPs, free IFNα (IFNα sn) or IFN-CT NPs. Data represents the mean ± S.E.M. of triplicates. Statistical significance is indicated with regard to control *Statistically significant difference ($p < 0.0001$).

Antiviral activity against HLTV-1. Two viral proteins were studied in PBMCs isolated from three patients naturally infected with different diseases associated with HTLV-1: (i) an infective dermatitis, (ii) a chronic ATL and (iii) an acute ATL. In cells from the chronic ATL and infective dermatitis patients, the percentage of cells expressing Tax protein did not decrease after any of the treatments (free or encapsulated IFNα), even with the highest dose. Noteworthy, chronic ATL patient was already under treatment with BIOFERON®. Consequently, only results corresponding to PBMCs from the acute ATL patient are shown in detail. Viral protein Tax was expressed in 46.2 ± 0.6% of untreated PBMCs from acute ATL patient. Significantly lower percentages were detected in cells treated with either IFNα (100 UI/mL: 33.97 ± 3.4%, 1000 UI/mL: 30.74 ± 1.0%, 10,000 UI/mL: 33.11 ± 0.2%) or IFN-CT NPs (100 UI/mL: 29.07 ± 3.8%; 1000 UI/mL: 32.14 ± 1.4%, 10,000 UI/mL: 33.11 ± 1.5%) with respect to the control, observing no differences between equal doses of each treatment or different doses of the same treatment (**Figure 3A**). Based on this, the intermediate dose (1000 UI/mL) was selected to perform the rest of the *in vitro* experiments involving PBMCs. In accordance with Tax determinations, in PBMCs from a dermatitis patient, the concentration of p19 in the supernatant was below the quantification limit. Conversely, the protein was quantified in culture supernatant of PBMCs from both ATL patients. The p19 concentration significantly decreased when treated either with free

or encapsulated IFNα. Data are shown for acute ATL patient, completing Tax determinations. Control cells secreted 1622 pg/mL, while IFNα and IFN-CT NPs treated cells secreted only 349 and 291 pg/mL, respectively ($p < 0.05$) (**Figure 3B**).

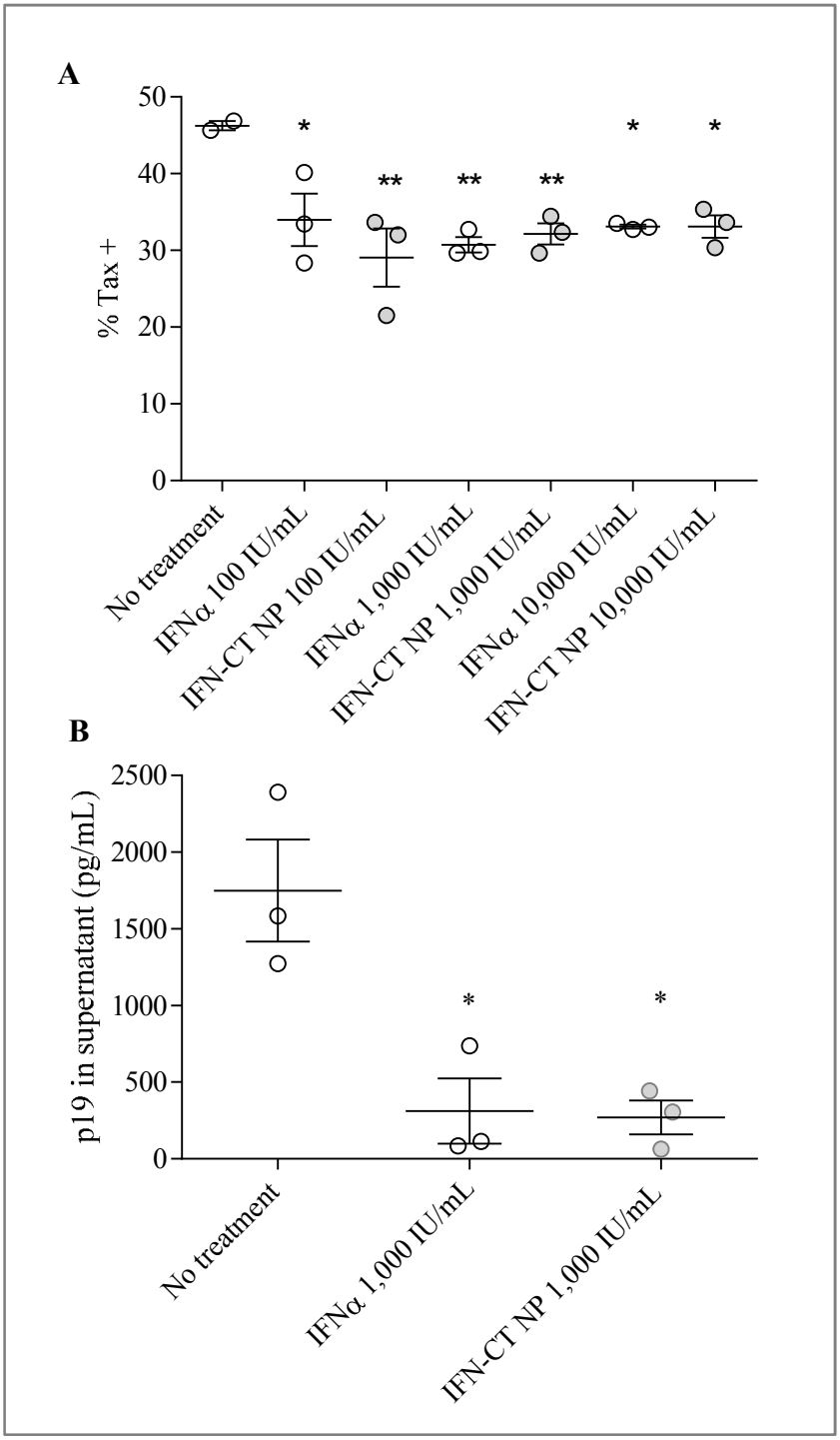

Figure 3. *In vitro* antiviral activity against HTLV-1. PBMCs from a patient with an Adult T Cell Leukemia (ATL) were treated with 100, 1000 or 10,000 IU/mL of free or encapsulated IFNα (IFN-CT NPs). (A) Percentage of cells expressing Tax viral protein and

(B) concentration of p19 viral protein. Results are expressed as mean ± S.E.M. (n = 3). Statistical significance is indicated with regard to control: *p <0.05 and **p <0.01.

Activation of IFNα signaling pathway. We compared the efficacy of IFNα and IFN-CT NPs in activating IFNα signaling pathways. First, PBMCs from healthy donors were studied. Expression of OAS1 in cells treated either with free IFNα or IFNα-loaded NPs differed significantly from the untreated control, while no significant difference was observed between them (IFNα: 26.99 ± 9.03-fold increase, IFN-CT NPs: 22.32 ± 7.24-fold increase; **Figure 4A**). Similarly, expression of RSAD2 was equally modulated by free IFNα and IFN-CT NPs (IFNα: 140.21 ± 12.72-fold increase, IFN-CT NPs: 153.61 ± 7.56-fold increase; **Figure 4B**). Then, PBMCs from a patient with acute ATL were used. In this case, a similar modulation was triggered by both treatments (135.9 ± 2.56-fold and 140.7 ± 17.65-fold increase for OAS1, respectively and 188.6 ± 10.2-fold increase and 141.7 ± 24.5-fold increase, respectively, for RSAD2).

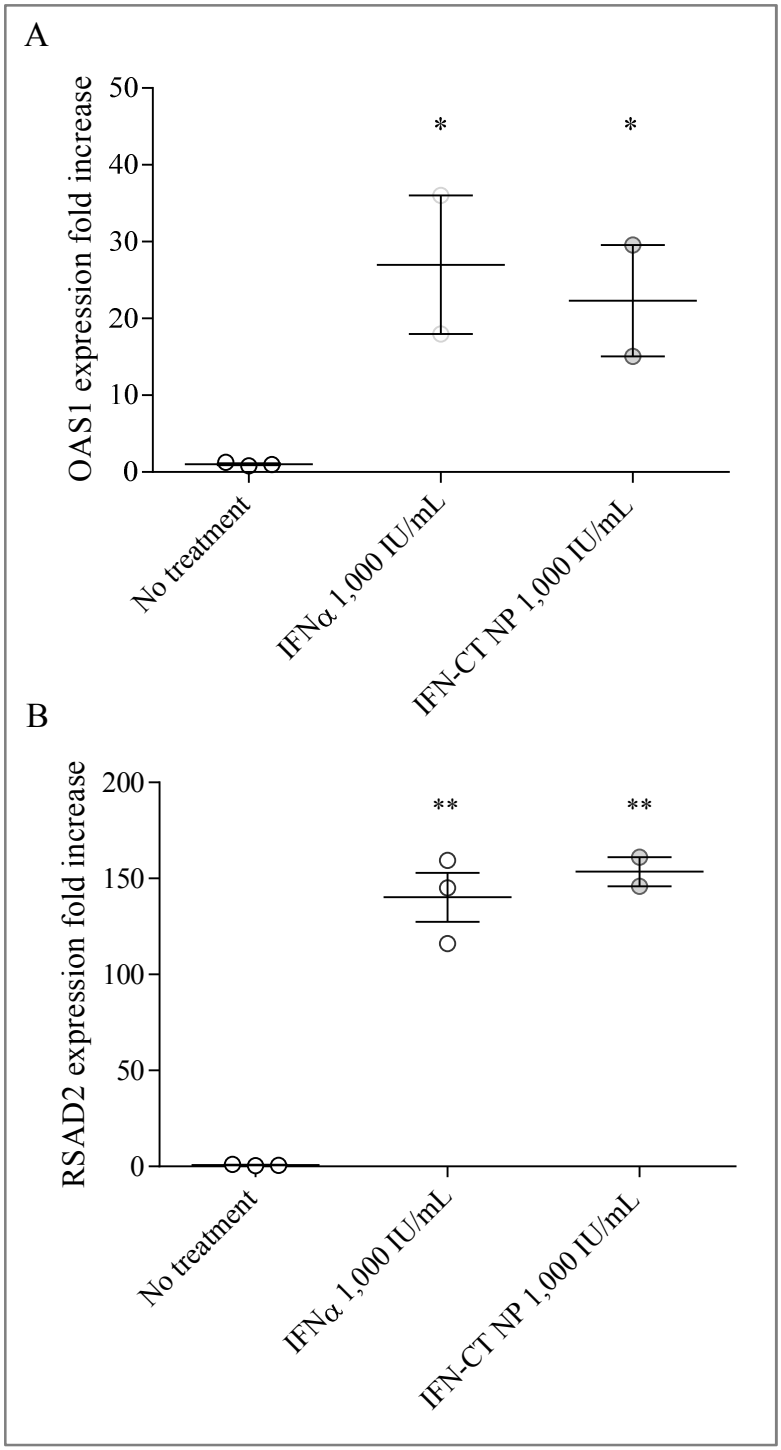

Figure 4. Expression level of IFN response genes in treated PBMCs. Copy DNA of two IFNα response genes: (A) 2'-5'-Oligoadenylate Synthase 1 (OAS1) and (B) Radical S-Adenosyl Methionine Domain Containing 2 (RSAD2). The mean ± S.E.M. of triplicates is

shown. Statistical significance is indicated with regard to control: *p <0.05 and **p <0.0001.

Overall, our results confirm that the nano-encapsulation of IFNα in CT nanoparticles does not jeopardize its antiviral activity *in vitro*, a remarkable advantage when compared to the pegylated derivatives.

Preliminary *in vivo* assay

Once we demonstrated the biological performance in several models of viral disease, we conducted the first preliminary *in vivo* evaluation, conducted in non-infected CF-1 mice. Outstandingly, the drug was detected in plasma in a concentration of 418.7 ± 280.2 pg/mL after 1 h of the oral administration of one single dose (0.3 MIU) of IFN-CT NPs. Conversely, at this time point, free IFNα could not be detected (**Figure 5**), in full agreement with studies conducted in mice, rabbit, dog and monkey[22,33,34]. Adverse effects are dose-dependent and thus, achieving pharmacologically active concentrations in plasma with lower doses would allow us to ensure therapeutic efficacy, while preventing them. This is why our results are very encouraging and open a new avenue to optimize the pharmacotherapy. To the best of our knowledge, this is the first time that a nanotechnology strategy of any kind enables the absorption of IFNα in the intestinal tract. Due to the relevance of the findings, future studies will comprise a full pharmacokinetic study employing larger animal groups.

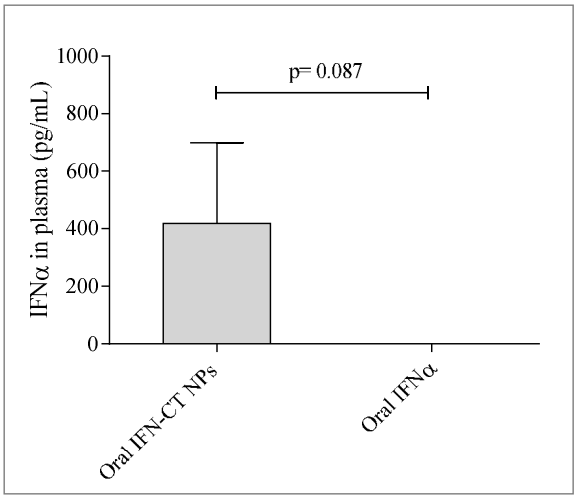

Figure 5. IFNα plasma concentration in CF-1 mice 1 h after oral administration of one single dose (0.3 MIU) of encapsulated (Oral IFN-CT NPs) or free IFNα (Oral IFNα). Data represents the mean ± S.E.M. of five samples. Statistical significance is indicated with regard to control: p=0.087.

CONCLUSIONS

In this study, we described the design and full characterization of a novel CT-based nanocarrier for the oral delivery of IFNα-2b aiming to replace its parenteral administration. The synthesis of the IFN-loaded nanoparticles is simple, reproducible and eventually scalable and the *%EE* almost 100%. The encapsulated drug conserved its antiviral activity, a remarkable advantage over pegylated counterparts that present a sharp activity loss. Finally, in a preliminary pharmacokinetic study, we demonstrated that these nanoparticles enhance the oral absorption of IFNα that could be detected in plasma, as opposed to the free derivative was undetectable. Overall results are promising and highlight the potential of this strategy to achieve an enhancement of both patient compliance and quality of life.

Furthermore, it can be translated to other cytokines and protein drugs in general. Ongoing studies will be devoted to characterize the oral pharmacokinetics in a relevant animal model.

Supporting Information. The Supporting Information is available free of charge on the ACS Publications website. Table S1: Clinical status of PBMCs donors infected with HTLV-1; Figure S1: *In vitro* drug release profile of IFN CT-NPs in media of bio-relevant pH.

AUTHOR INFORMATION

canepa.camila@gmail.com (Camila Cánepa), julietaimperiale@gmail.com (Julieta C. Imperiale), cberini@fmed.uba.ar (Carolina A. Berini), vetmarianelalewicki@gmail.com (Marianela Lewicki), sosnik@technion.ac.il, alesosnik@gmail.com (Alejandro Sosnik), mbiglione@fmed.uba.ar (Mirna M. Biglione).

Corresponding Author

*mbiglione@fmed.uba.ar

Author Contributions

CC carried out the experiments. JCI performed the quantification of free CT, FTIR analysis and helped to conceive and plan the totality of the experiments. CB helped to carry out the ELISAs and to process HTLV-1 infected patient blood samples. ML manipulated mice for drug administration and blood sample extraction. AS and MB equally contributed to conceive the original idea and supervised the project. All authors contributed to the

interpretation of the results, provided critical feedback and helped to carry out the different stages of the research. The manuscript was written through contributions of all authors, who have given approval to the final version of the manuscript.

FUNDING SOURCES

Grant provided by the National Agency for Scientific and Technological Promotion (PICT N° 2012-0322) - Grant provided by the National Scientific and Technical Research Council (PIP N° 112 20110100644).

ACKNOWLEDGMENTS. We thank BIOARS S.A. (Argentina) for providing the ELISA kit for the diagnosis of HTLV infection. We are grateful to Prof. Paul Fisch (Institute of Clinical Pathology, University of Freiburg, Germany) for providing the ELISA kit for IFN quantification and to Prof. Tanaka Yuetsu (Department of Immunology, School of Medicine, University of the Ryukyus, Japan) for kindly providing the mouse monoclonal antibody (mAb) against Tax. We also thank Dr. Magdalena Gherardi for their precious assistance in the *in vivo* experiments.

ABBREVIATIONS

IFNα: interferon alpha; IFN-CT NPs: IFNα-2b-loaded chitosan nanoparticles; HLTV-1: Human Lymphotropic-T Virus type 1; DLS: dynamic light scattering; TEM: transmission electron microscopy; PEG-IFNα: pegylated form of IFNα; ATL: Adult T Cell Leukemia; CT: chitosan; TPP: sodium tripolyphosphate pentabasic. D_h: hydrodynamic diameter; PDI: polydispersity index; ATR/FTIR: Attenuated total reflectance / Fourier transform infrared spectroscopy; *%EE:* encapsulation efficiency; PBMCs: peripheral blood mononuclear cells.

PMA: phorbol 12-myristate 13-acetate; VSV Vesicular Stomatitis Virus; mAb: mouse monoclonal antibody. CICUAL: Institutional Committee for Care and Use of Experimental Animals; OAS1: 2'-5'-Oligoadenylate Synthase 1; RSAD2: Radical S-Adenosyl Methionine Domain Containing 2; PEG: poly(ethylene glycol); FDA: Food and Drug Administration; GRAS: Generally Recognized As Safe.

REFERENCES

1. Griffin, B. T.; Guo, J.; Presas, E.; Donovan, M. D.; Alonso, M. J.; O'Driscoll, C. M., Pharmacokinetic, pharmacodynamic and biodistribution following oral administration of nanocarriers containing peptide and protein drugs. *Adv Drug Delivery Rev* **2016,** *106* (Pt B), 367-380.
2. Shah, R. B.; Ahsan, F.; Khan, M. A., Oral delivery of proteins: progress and prognostication. *Crit Rev Ther Drug Carrier Syst* **2002,** *19* (2), 135-69.
3. Fonte, P.; Araujo, F.; Reis, S.; Sarmento, B., Oral insulin delivery: how far are we? *J Diabetes Sci Technol* **2013,** *7* (2), 520-31.
4. Aguirre, T. A.; Teijeiro-Osorio, D.; Rosa, M.; Coulter, I. S.; Alonso, M. J.; Brayden, D. J., Current status of selected oral peptide technologies in advanced preclinical development and in clinical trials. *Adv Drug Delivery Rev* **2016,** *106* (Pt B), 223-241.
5. Brayden, D. J.; Alonso, M. J., Oral delivery of peptides: opportunities and issues for translation. *Adv Drug Delivery Rev* **2016,** *106* (Pt B), 193-195.
6. Bruno, B. J.; Miller, G. D.; Lim, C. S., Basics and recent advances in peptide and protein drug delivery. *Ther Delivery* **2013,** *4* (11), 1443-67.
7. Chung, H.; Kim, J.; Um, J. Y.; Kwon, I. C.; Jeong, S. Y., Self-assembled "nanocubicle" as a carrier for peroral insulin delivery. *Diabetologia* **2002,** *45* (3), 448-51.
8. Foss, A. C.; Goto, T.; Morishita, M.; Peppas, N. A., Development of acrylic-based copolymers for oral insulin delivery. *Eur J Pharm Biopharm* **2004,** *57* (2), 163-9.
9. Pan, Y.; Li, Y. J.; Zhao, H. Y.; Zheng, J. M.; Xu, H.; Wei, G.; Hao, J. S.; Cui, F. D., Bioadhesive polysaccharide in protein delivery system: chitosan nanoparticles improve the intestinal absorption of insulin in vivo. *Int J Pharm* **2002,** *249* (1-2), 139-47.
10. Oppenheim, R. C., The Production and Evaluation of Orally Administered Insulin Nanoparticles. Drug Dev Ind Pharm **1982,** *8* (4), 531-546.
11. Constantinides, P. P., Lipid microemulsions for improving drug dissolution and oral absorption: physical and biopharmaceutical aspects. *Pharm Res* **1995,** *12* (11), 1561-72.
12. Yoshida, H., Niosomes for oral delivery of peptide drugs. *J Controlled Release* **1992,** *21* (1-3), 145-153.
13. Gupta, S.; Jain, A.; Chakraborty, M.; Sahni, J. K.; Ali, J.; Dang, S., Oral delivery of therapeutic proteins and peptides: a review on recent developments. *Drug Delivery* **2013,** *20* (6), 237-46.
14. Spiegel, R. J., Intron A (interferon alfa-2b): clinical overview and future directions. *Semin Oncol* **1986,** *13* (3 Suppl 2), 89-101.
15. Asmana Ningrum, R., Human interferon alpha-2b: a therapeutic protein for cancer treatment. *Scientifica (Cairo)* **2014,** *2014*, 970315.

16. Youngster, S.; Wang, Y. S.; Grace, M.; Bausch, J.; Bordens, R.; Wyss, D. F., Structure, biology, and therapeutic implications of pegylated interferon alpha-2b. *Curr Pharm Des* **2002,** *8* (24), 2139-57.
17. Bazarbachi, A.; Plumelle, Y.; Carlos Ramos, J.; Tortevoye, P.; Otrock, Z.; Taylor, G.; Gessain, A.; Harrington, W.; Panelatti, G.; Hermine, O., Meta-analysis on the use of zidovudine and interferon-alfa in adult T-cell leukemia/lymphoma showing improved survival in the leukemic subtypes. *J Clin Oncol* **2010,** *28* (27), 4177-83.
18. Aghdam, A. G., Bioconjugation of Interferon-alpha Molecules to Lysine-Capped Gold Nanoparticles for Further Drug Delivery Applications. *J Dispersion Sci Technol* **2008,** *29* (8), 1062-1065
19. Lesinski, G. B.; Sharma, S.; Varker, K. A.; Sinha, P.; Ferrari, M.; Carson, W. E., 3rd, Release of biologically functional interferon-alpha from a nanochannel delivery system. *Biomed Microdevices* **2005,** *7* (1), 71-9.
20. Kondiah, P. P.; Tomar, L. K.; Tyagi, C.; Choonara, Y. E.; Modi, G.; du Toit, L. C.; Kumar, P.; Pillay, V., A novel pH-sensitive interferon-beta (INF-beta) oral delivery system for application in multiple sclerosis. *Int J Pharm* **2013,** *456* (2), 459-72.
21. Muzzarelli, R. A., Colorimetric determination of chitosan. *Anal Biochem* **1998,** *260* (2), 255-7.
22. Wills, R. J.; Spiegel, H. E.; Soike, K. F., Pharmacokinetics of recombinant alpha A interferon following I.V. infusion and bolus, I.M., and P.O. administrations to African green monkeys. *J Interferon Res* **1984,** *4* (3), 399-409.
23. Shah, L. K.; Amiji, M. M., Intracellular delivery of saquinavir in biodegradable polymeric nanoparticles for HIV/AIDS. *Pharm Res* **2006,** *23* (11), 2638-45.
24. European Pharmacopoeia **2005,** *5th Revised edition*.
25. Desai, K. G., Chitosan Nanoparticles Prepared by Ionotropic Gelation: An Overview of Recent Advances. *Crit Rev Ther Drug Carrier Syst* **2016,** *33* (2), 107-58.
26. Dong, Y.; Ng, W. K.; Shen, S.; Kim, S.; Tan, R. B., Scalable ionic gelation synthesis of chitosan nanoparticles for drug delivery in static mixers. *Carbohydr Polym* **2013,** *94* (2), 940-5.
27. Sainz, V.; Conniot, J.; Matos, A. I.; Peres, C.; Zupancic, E.; Moura, L.; Silva, L. C.; Florindo, H. F.; Gaspar, R. S., Regulatory aspects on nanomedicines. *Biochem Biophys Res Commun* **2015,** *468* (3), 504-10.
28. He, C.; Yin, L.; Tang, C.; Yin, C., Size-dependent absorption mechanism of polymeric nanoparticles for oral delivery of protein drugs. *Biomaterials* **2012,** *33* (33), 8569-78.
29. Win, K. Y.; Feng, S. S., Effects of particle size and surface coating on cellular uptake of polymeric nanoparticles for oral delivery of anticancer drugs. *Biomaterials* **2005,** *26* (15), 2713-22.
30. Zhao, S.; Liu, E.; Chen, P.; Cheng, D.; Lu, S.; Yu, Q.; Wang, Y.; Wei, K.; Yang, P., A comparison of peginterferon alpha-2a and alpha-2b for treatment-naive patients with chronic hepatitis C virus: A meta-analysis of randomized trials. *Clin Ther* **2010,** *32* (9), 1565-77.
31. Thomas, T.; Foster, G., Nanomedicines in the treatment of chronic hepatitis C--focus on pegylated interferon alpha-2a. *Int J Nanomedicine* **2007,** *2* (1), 19-24.
32. Chirkov, S. N., [The antiviral activity of chitosan (review)]. *Prikl Biokhim Mikrobiol* **2002,** *38* (1), 5-13.
33. Cantell, K.; Hirvonen, S.; Pyhala, L.; De Reus, A.; Schellekens, H., Circulating interferon in rabbits and monkeys after administration of human gamma interferon by different routes. *J Gen Virol* **1983,** *64 (Pt 8)*, 1823-6.
34. Gibson, D. M.; Cotler, S.; Spiegel, H. E.; Colburn, W. A., Pharmacokinetics of recombinant leukocyte A interferon following various routes and modes of administration to the dog. *J Interferon Res* **1985,** *5* (3), 403-8.

For Table of Contents Use Only

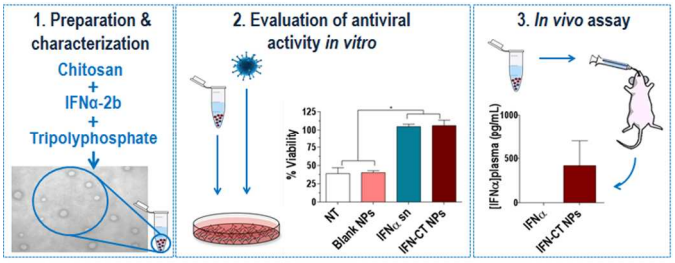

Development of a drug delivery system based on chitosan nanoparticles for oral administration of interferon-alpha

Camila Cánepa, Julieta C. Imperiale, Carolina A. Berini, Marianela Lewicki, Alejandro Sosnik & Mirna M. Biglione

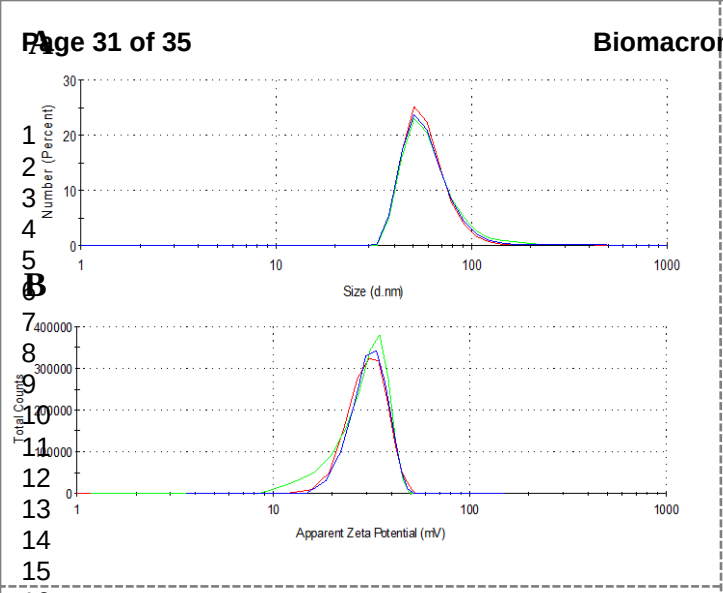
A
Number (Percent)
Size (d.nm)
B
Total Counts
Apparent Zeta Potential (mV)

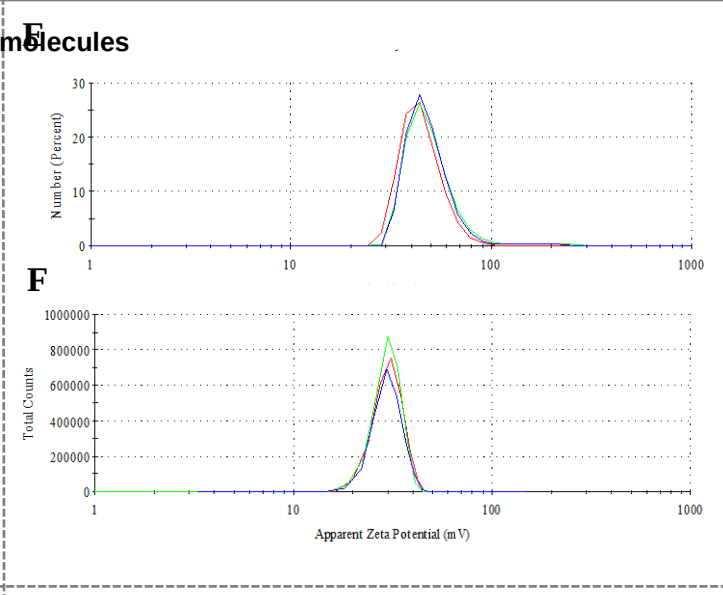
E
Number (Percent)
F
Total Counts
Apparent Zeta Potential (mV)

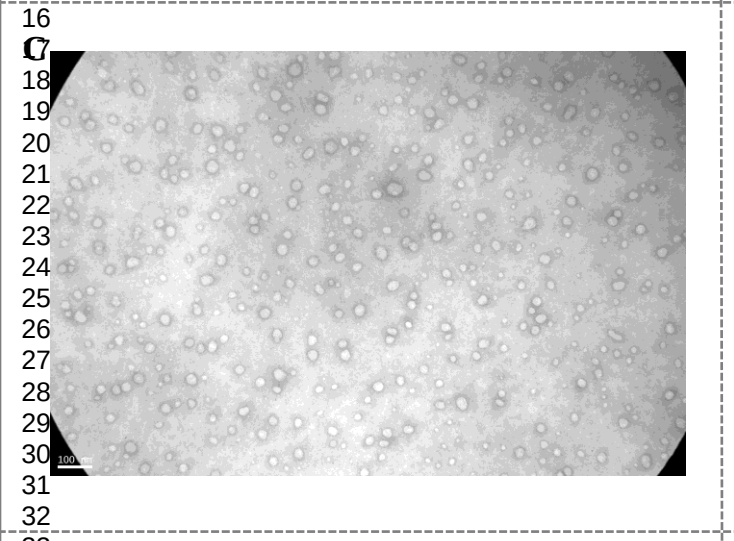
C
100 nm

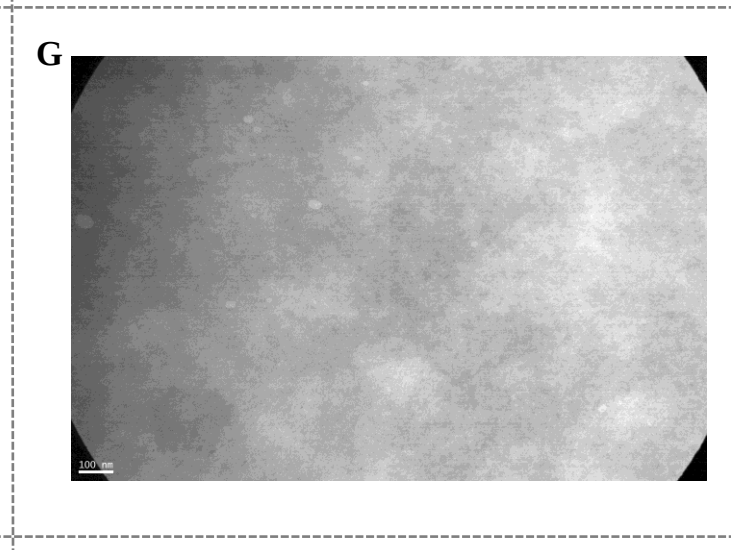
G
100 nm

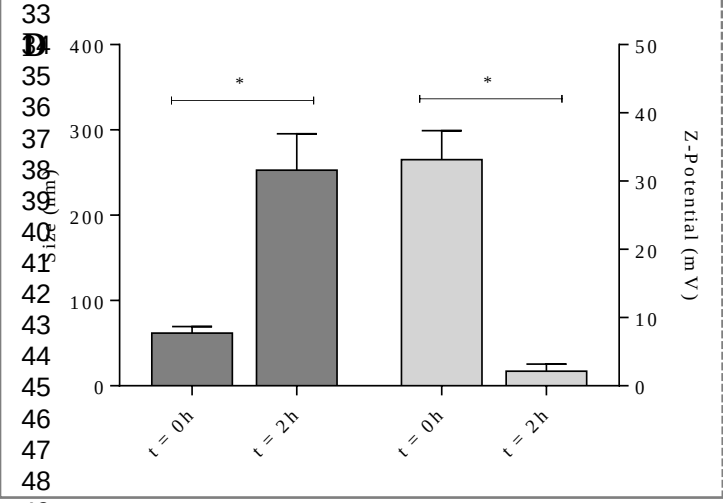
D
Size (nm)
Z-Potential (mV)
t = 0h
t = 2h
t = 0h
t = 2h

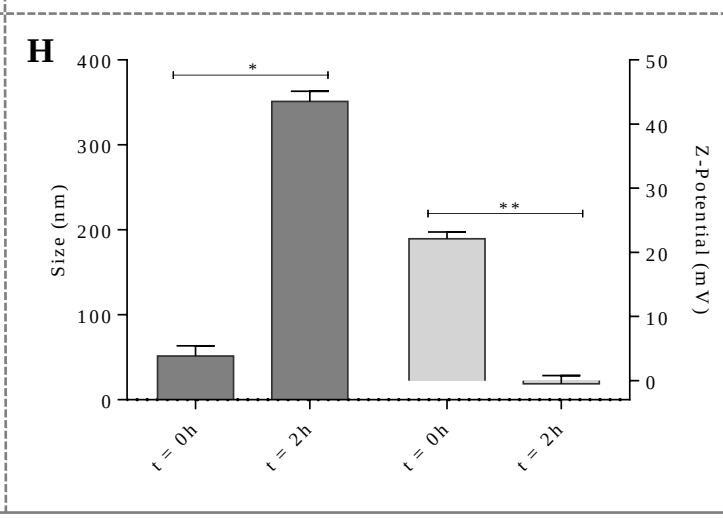
H
Size (nm)
Z-Potential (mV)
t = 0h
t = 2h
t = 0h
t = 2h

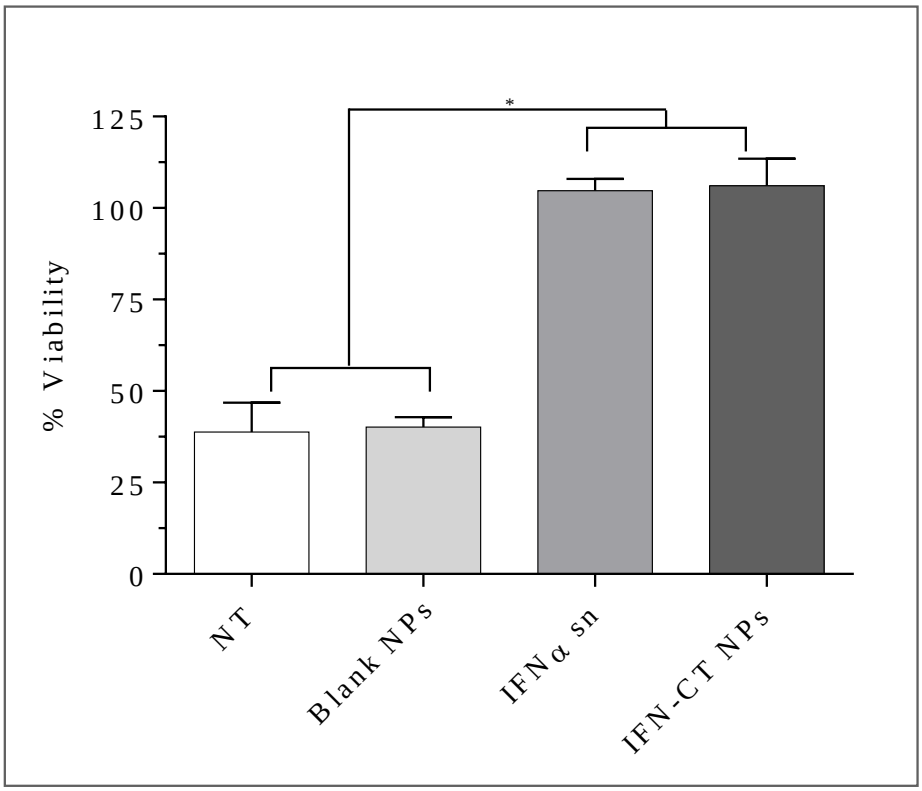
*
125
100
75
50
25
0
% Viability
NT
Blank NPs
IFNα sn
IFN-CT NPs

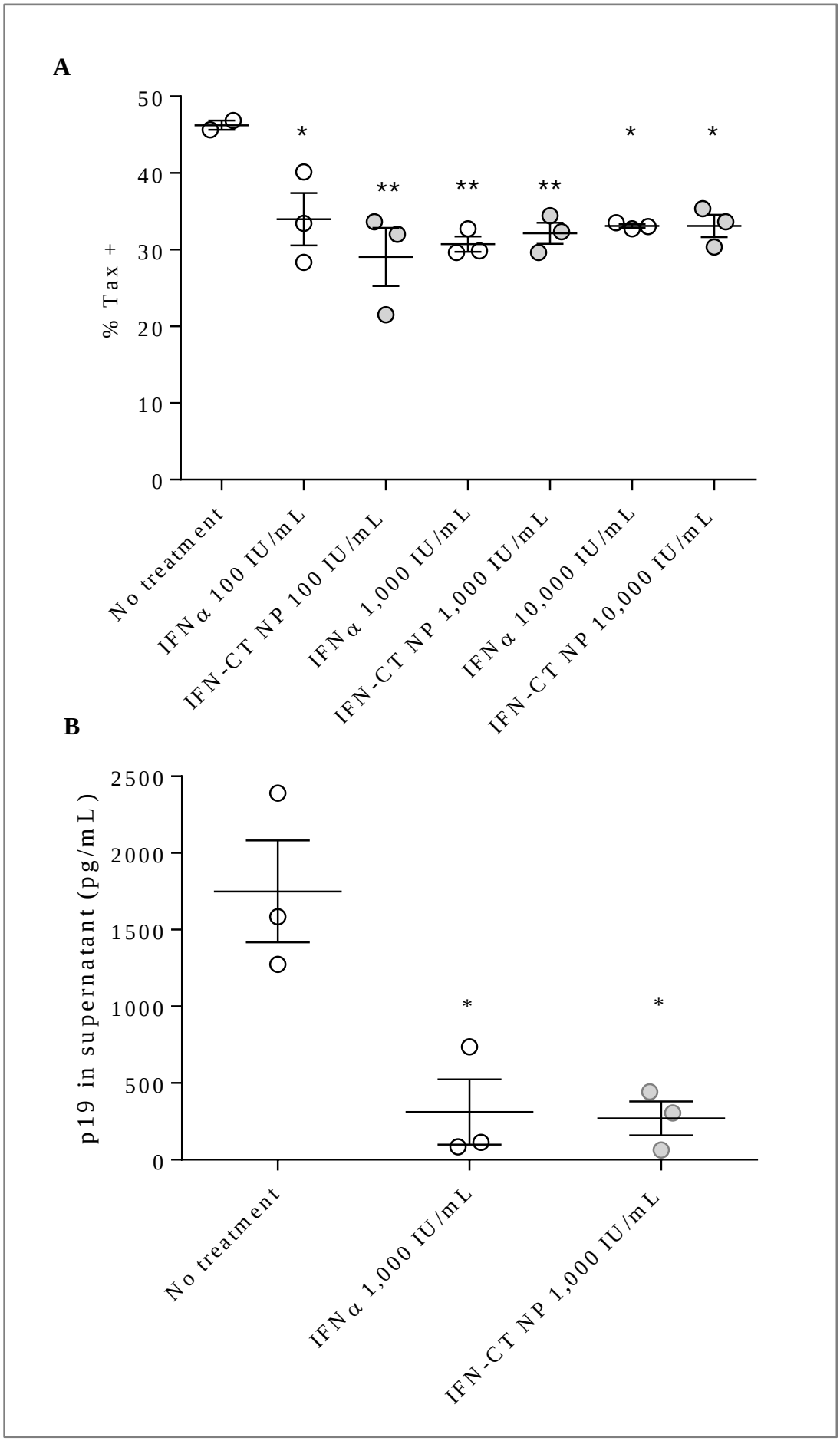
A
% Tax +
50
40
30
20
10
0
*
**
**
**
*
*
No treatment
IFNα 100 IU/mL
IFN-CT NP 100 IU/mL
IFNα 1,000 IU/mL
IFN-CT NP 1,000 IU/mL
IFNα 10,000 IU/mL
IFN-CT NP 10,000 IU/mL
B
p19 in supernatant (pg/mL)
2500
2000
1500
1000
500
0
*
*
No treatment
IFNα 1,000 IU/mL
IFN-CT NP 1,000 IU/mL

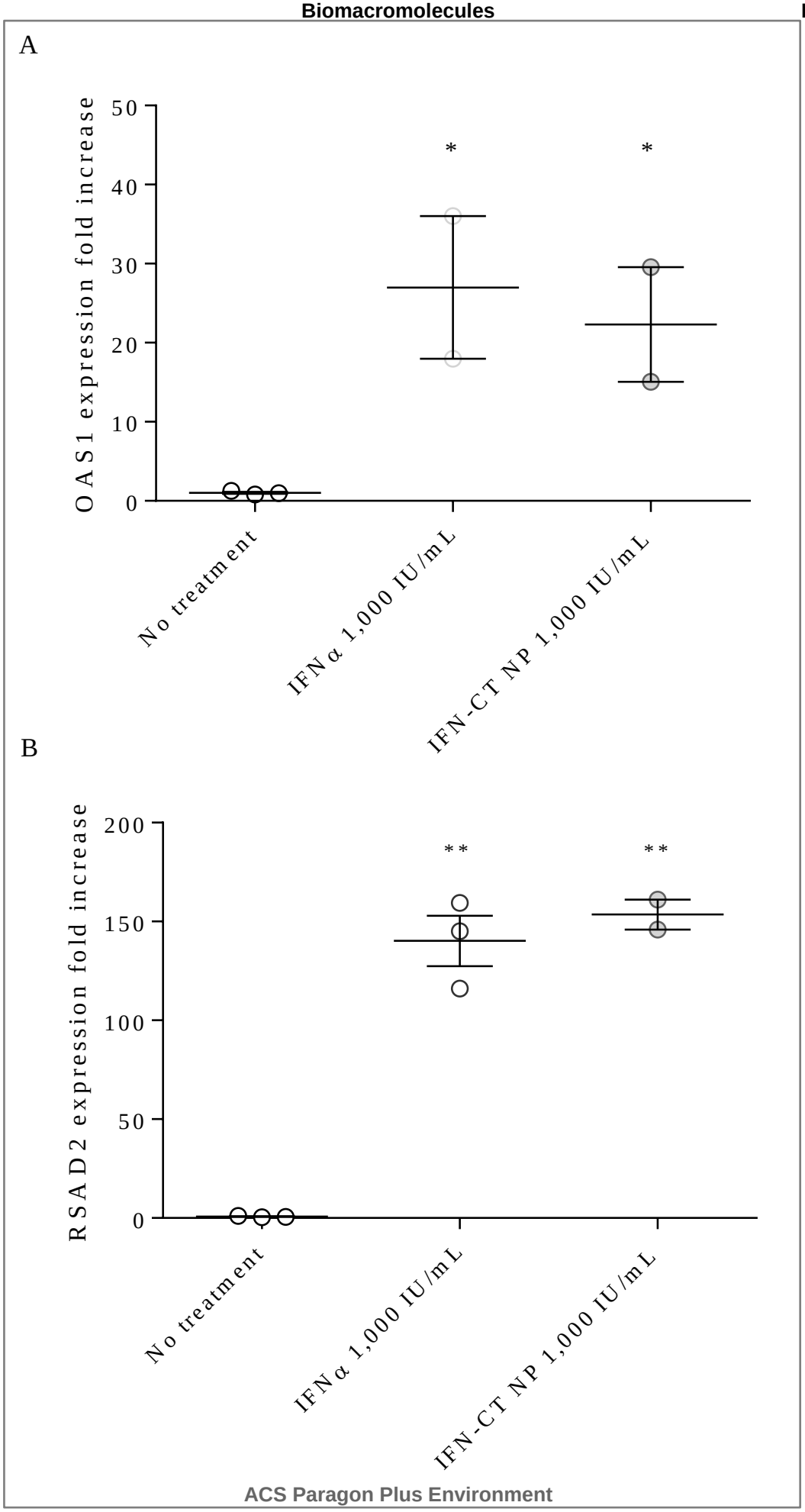
A
OAS1 expression fold increase
50
40
30
20
10
0
*
*
No treatment
IFNα 1,000 IU/mL
IFN-CT NP 1,000 IU/mL
B
RSAD2 expression fold increase
200
150
100
50
0
**
**
No treatment
IFNα 1,000 IU/mL
IFN-CT NP 1,000 IU/mL

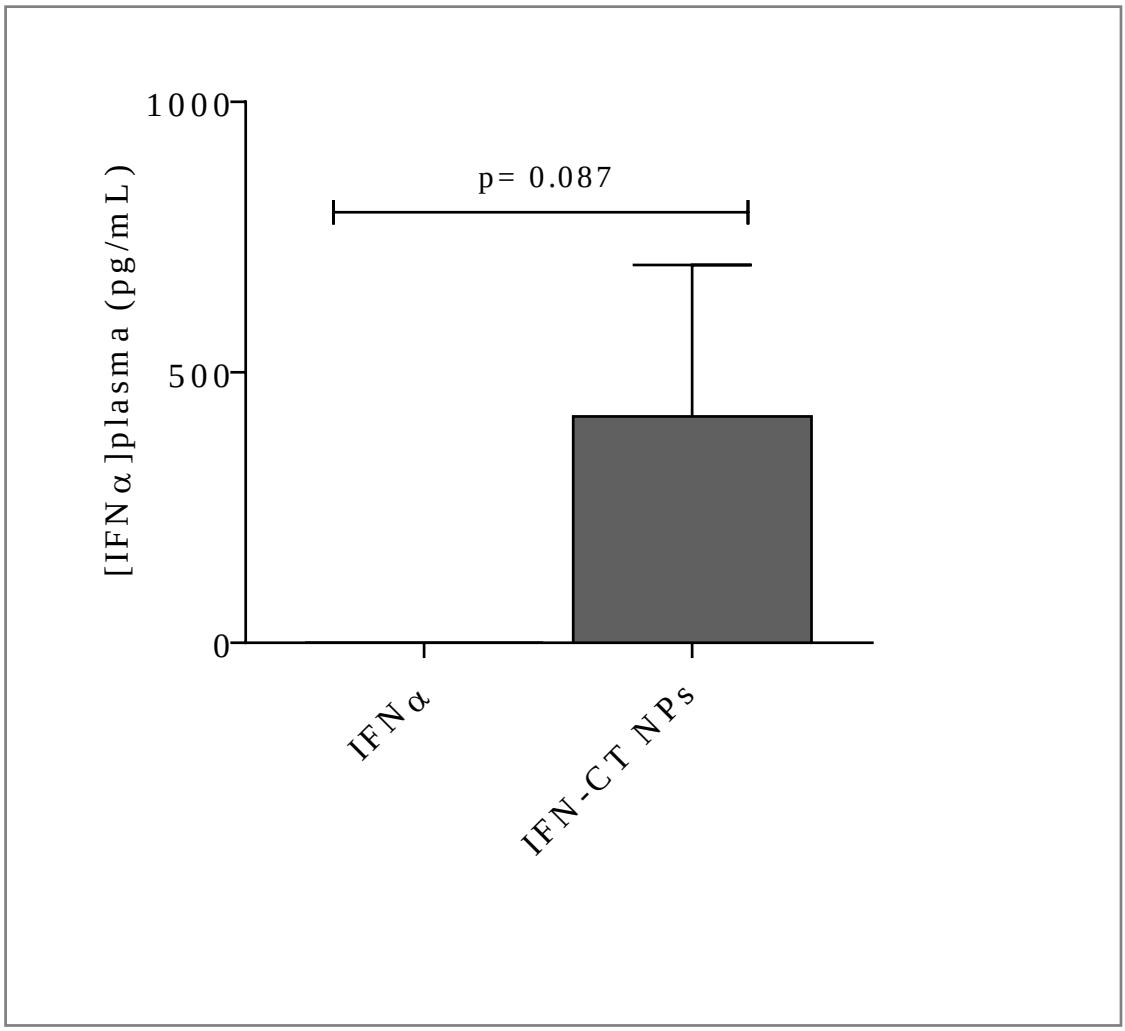
1000
500
0
[IFNα]plasma (pg/mL)
p= 0.087
IFNα
IFN-CT NPs